2016 IEEE International Conference on Robotics and Automation (ICRA)
Stockholm, Sweden, May 16-21, 2016

Optimal Configuration of Series and Parallel Elasticity in a 2D Monoped

Yevgeniy Yesilevskiy, Zhenyu Gan and C. David Remy, *Member, IEEE*

***Abstract*— This paper uses optimal control to simultaneously optimize the motion and morphology of a realistic model of a 2D Monoped. In particular, we compare the energetics of four different actuator configurations: a parallel elastic actuator (PEA) in the hip and a series elastic actuator in the leg (SEA), series hip and parallel leg, series hip and series leg, and parallel hip and parallel leg. We use realistic models with mass in the legs and feet, damping in the springs, and detailed DC electric motor models. The comparison is carried out for the cost of transport of three energetic measures: positive motor work, electrical losses, and positive electrical work, and evaluated as a function of velocity. In our optimization we include motor parameters, stiffness, and spring pre-compression terms as free variables, ensuring that we compare the energetically optimal version of each configuration at each velocity. We show that for the positive motor work and the electrical losses costs of transport (COT), the parallel hip and series leg configuration is energetically optimal. For the electrical work, the optimal configuration is speed dependent, with series hip and parallel leg optimal at low speeds, and both series hip series leg and parallel hip series leg optimal at high speeds.**

I. Introduction

The way that a legged system is built and the way that it moves are fundamentally connected. This connection is readily apparent when a legged robot moves in a way that maximizes its energetic economy. Model based studies have shown that robots moving in this way take advantage of their *natural dynamics* [1], [2] (the intrinsic morphologically based motions that result from the interplay of gravity, inertia, and elasticity in the springs). For these models, springs play a key role in explaining the dynamics of legged systems.

Motivated by nature [3], [4] and the passive dynamic results above, we include elasticity in our models. To understand the energetic considerations of a particular morphology, we also incorporate actuators. In doing so, we now alter the passive structure of the robot, and consequently, alter the way in which the legged system moves efficiently. The optimal motion is further complicated by the fact that we have many different choices on how to implement the actuators, and, that different motor and spring parameters are ideal for each case. The two most common implementations are to place the springs either in series (Series Elastic Actuator, SEA) or in parallel (Parallel Elastic Actuator, PEA) with the motor. The primary advantage of SEA is that the motor inertia is coupled by a spring to the joint inertia. As a result, the motor is well isolated from impacts, and the motor inertia does not interfere with the joint motion. The primary advantage for PEA is that the motor force and the parallel spring force act additively, which can decrease the force requirements on the motor.

The authors are with the Robotics and Motion Laboratory (RAMlab), Department of Mechanical Engineering, University of Michigan, Ann Arbor, MI (yevyes@umich.edu, ganzheny@umich.edu, cdremy@umich.edu). This material is based upon work supported by the National Science Foundation under Grant No. 1453346.

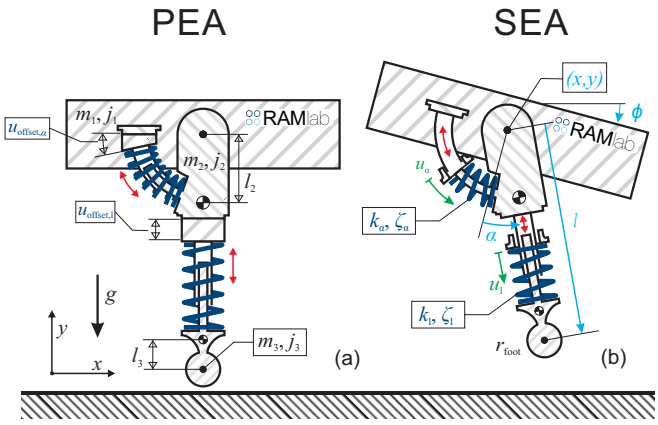

Fig. 1. In this paper we use optimal control to find the most energetically economical configuration of actuators on a two-dimensional monoped. We compare four configurations, a parallel elastic actuator (PEA) at both the hip and the leg (shown on the left), a series elastic actuator (SEA) at both locations (shown on the right), a SEA at the hip and PEA at the leg, and a PEA at the hip and an SEA at the leg. In the optimization, we simultaneously optimize for the motion and morphology of each configuration to ensure that we compare the best possible version of each monoped. Our models have mass in the legs and feet, damping, and realistic DC electric motor models. We additionally include realistic constraints on the leg length, motor force, and motor velocity.

In this paper we seek to find the optimal configuration of SEA and PEA in a two-dimensional monoped. While in the past we have worked with one-dimensional monopedal hopping [5], moving to a second dimension greatly increases the complexity of the problem. Both the hip and the leg can have either PEA or SEA, leading to four possible actuator configurations. The two-dimensional monoped moves with a forward velocity, which leads to much more complex motions that require careful coordination between the hip and leg. The parameter space over which to optimize morphology is greatly expanded by the addition of a second motor and spring. Lastly, and perhaps most importantly, we are optimizing for the motion and parameters of actuators that have very different roles in legged locomotion. The hip actuator coordinates the leg swing dynamics, while the leg springs mimics the behavior of a spring loaded inverted pendulum (SLIP) [6].

We seek motions that minimize the cost of transport (COT) (the amount of energy divided by the distance traveled [7], [8]), for three separate cost functions: the positive motor

Authorized licensed use limited to: Technische Universitaet Muenchen. Downloaded on December 30,2021 at 10:34:46 UTC from IEEE Xplore. Restrictions apply.

work, electrical losses, and the positive electrical work. Utilizing our prior results [5] and previous model-based studies [9], we hypothesize that the optimal configuration will be cost function dependent. For the positive motor work and positive electrical work costs of transport (COT), we predict that the optimal configuration will have a series leg, as a SEA was energetically optimal for the one-dimensional hopper. For the electrical losses COT, we predict that the optimal configuration will have a parallel leg, as PEA was slightly more economical for in-place hopping. For all three cost functions, we hypothesize that the two-dimensional monoped will favor a parallel hip. This prediction is motivated by [10], who found periodic walking gaits on flat ground with no energy input. As there is no active input in their bipedal model, the hip spring acts entirely to time the swing leg dynamics passively. A PEA with no torque applied mimics this situation. Therefore, we predict that with an optimal stiffness, the parallel spring should largely account for leg swing timing.

By systematically testing these hypotheses, we show the possibility of using optimization to make design choices on a realistic robot model performing a realistic task. While our work on the one-dimensional hopper [5] showed how optimization can be used to compare two distinct legged robot morphologies, the task was intentionally simplified to allow us to ensure our methodology worked. The two-dimensional motion optimized for here represents the motion that each leg of a biped undergoes during running, with all the complexities of swing-leg coordination. Furthermore, the choice of actuator is an open question in hardware and simulation. ScarlETH has SEA in both the hip and the knee [11]. MABEL also makes use of SEA [12] while Phides utilizes PEA [13]. In prosthetics, the effect of parallel and series elasticity has also been studied on an ankle joint [14]. In simulation, [15] compare PEA and SEA for stationary hopping and conclude that PEA is more energetically efficient for typical robotic properties and motions. This work, however, only looks at the electrical losses, ignores losses during flight, ignores collision losses, and does not include a detailed electric motor model. With this present work, we include these missing aspects and we show how our previous methodology can be extended to compare different configurations of SEA and PEA in order choose the most energetically economical structure.

To make our optimization procedure relevant for actual hardware design choices, we use realistic models. These models have mass in the feet and upper leg, realistic DC electric motor models, and damping in the springs. The models have realistic constraints on torques, velocities, leg lengths, and all parameter values. In these optimizations we include the stiffness and motor parameters as free variables. In this way we ensure that the optimizer is allowed to choose the best morphology for a particular actuator configuration. We show that the optimal configuration depends on the velocity as well as the cost function. The optimal configuration is primarily driven by damping losses and negative actuator work, with collisions playing a comparatively small role.

II. Methods

A. Model

The 2D monoped models in this study (Fig. 1) are similar to our previous models [9], [16]. In this section we extend the equations of motion to include PEA. Each model includes three rigid bodies: the main body, upper limb, and lower limb. The main body has a mass of m_1 and an inertia of j_1, with the hip joint located at the center of mass (COM). It has three degree of freedoms: its horizontal and vertical position x, y and orientation ϕ. The upper limb segment connects to the main body via a rotational hip joint. It has a mass of m_2 and an inertia of j_2. Its COM is located at a distance l_2 from the hip joint. The lower limb segment, which moves relative to the upper limb through a prismatic knee joint, has mass m_3 and inertia j_3. The COM is located a distance l_3 away from the center of the foot. The remaining model states are the angle of the leg, α, and the length of the leg, l, which is measured from the COM of the main body to the center of the foot.

In contrast to our previous work [9], in this model both the hip joint and knee joint can either have PEA or SEA to control the desired motion. These models are therefore the two-dimensional extension of our previous work on one-dimensional hoppers [5]. If PEA is chosen for the hip joint, the rotational hip spring is rigidly attached to the upper leg segment at one end and to the main body at the other end with an offset angle $u_{offset,\alpha}$ (this spring pre-compression is introduced to keep the comparison between SEA and PEA fair). The hip torque is the sum of the torque produced by the spring and the motor:

$$T_P = k_\alpha(\alpha_o + u_{offset,\alpha} - \alpha) + b_\alpha\dot{\alpha} + T_{mot} \qquad (1)$$

Where α_o is the rest angle of the hip spring. Similarly, for the knee joint:

$$F_P = k_l(l_o + u_{offset,l} - l) + b_l\dot{l} + F_{mot} \qquad (2)$$

Where l_o is the rest length of the leg spring.

For SEA, the motor force is equal to the force produced by the spring. Here the hip spring is connected directly to the hip motor on one end, and connected to the upper limb at the other end. The motor position of the hip, u_α, is introduced as an additional generalized coordinate. Similarly, for the leg, the motor position u_l is an additional generalized coordinate. These displacements are driven by the motor torques τ_α and τ_l. The joint forces for the hip and knee joints become:

$$T_S = k_\alpha(\alpha_o + u_\alpha - \alpha) + b_\alpha(\dot{u_\alpha} - \dot{\alpha}) = T_{mot} \qquad (3)$$

$$F_S = k_l(l_o + u_l - l) + b_l(\dot{u_l} - \dot{l}) = F_{mot} \qquad (4)$$

The damping coefficients b_l and b_α are obtained from desired damping ratios ζ_l and ζ_α. Based on the selection of the actuators, four different configurations are tested in the following section for optimal performance (PEA-hip and PEA-leg, PEA-hip and SEA-leg, SEA-hip and PEA-leg, SEA-hip and SEA-leg). The number of generalized coordinates for the model depends on the particular configuration being chosen.

Authorized licensed use limited to: Technische Universitaet Muenchen. Downloaded on December 30,2021 at 10:34:46 UTC from IEEE Xplore. Restrictions apply.

TABLE I

MODEL PARAMETERS AND LIMITS EXPRESSED WITH RESPECT TO THE TOTAL MASS m_o, LEG LENGTH l_o, AND GRAVITY g. ALL VALUES ARE BASED ROUGHLY ON PAST PROTOTYPES [11].

m_1 = 0.7 m_o	j_1 = 0.4 $m_o l_o^2$	l_{min} = 0.5 l_o	$c_{lim,\alpha}$ = 0.091
m_2 = 0.2 m_o	j_2 = 0.004 $m_o l_o^2$	l_{max} = 1.15 l_o	$c_{lim,l}$ = 0.091
m_3 = 0.1 m_o	j_3 = 0.004 $m_o l_o^2$	$u_{min,l}$ = -0.15 l_o	ζ_α = 0.2
$k_{min,l}$ = 0.0001 $m_o g/l_o$	l_o = 1 l_o	$u_{max,l}$ = 0.15 l_o	ζ_l = 0.2
$k_{max,l}$ = 1000 $m_o g/l_o$	l_2 = 0.25 l_o	$u_{min,\alpha}$ = $-\pi/4$	$\bar{u}_{min,l}$ = 0.0001 $\sqrt{l_o g}$
$k_{min,\alpha}$ = 0.0001 $m_o g/l_o$	l_3 = 0.25 l_o	$u_{max,\alpha}$ = $\pi/4$	$\bar{u}_{max,l}$ = 10 $\sqrt{l_o g}$
$k_{max,\alpha}$ = 1000 $m_o g/l_o$	$P_{max,\alpha}$ = 9.4 $m_o g\sqrt{g l_o}$	$j_{unsc,l}$ = 0.251 $m_o g l_o$	$\bar{u}_{min,\alpha}$ = 0.0001 $\sqrt{l_o g}$
r_{foot} = 0.05 l_o	$P_{max,l}$ = 9.4 $m_o g\sqrt{g l_o}$	$j_{unsc,\alpha}$ = 0.251 $m_o g l_o$	$\bar{u}_{max,\alpha}$ = 10 $\sqrt{l_o g}$

To keep the following analysis general, all states and parameters are normalized with respect to the total mass m_o, gravity g, and relaxed leg length l_o. The values of all of the parameters we use in this study and their bounds are shown in Table I (these are roughly obtained from previous hardware [11]).

B. System Dynamics

As described before, the total number of generalized coordinates depends on the type of actuator chosen for each joint. For example, if PEA is chosen for the hip and SEA for the knee joint, the generalized coordinates are $\mathbf{q} = [x, y, \phi, \alpha, l, u_l]^T$ and the generalized forces are $\boldsymbol{\tau} = [0, 0, 0, T_P, F_S, \tau_l - F_S]^T$. The continuous dynamics of the model are governed by the equations of motion (*EOM*) which are stated in the canonical form [17]:

$$\mathbf{M}(\mathbf{q})\ddot{\mathbf{q}} + \mathbf{h}(\mathbf{q},\ \dot{\mathbf{q}}) = \boldsymbol{\tau} + \mathbf{J}^T(\mathbf{q})\boldsymbol{\lambda}, \tag{5}$$

where $\mathbf{M}(\mathbf{q})$ is the mass matrix and $\mathbf{h}(\mathbf{q},\ \dot{\mathbf{q}})$ represents the Coriolis, centrifugal, and gravitational terms. The contact Jacobian $\mathbf{J}$ maps the vector of contact forces λ into the generalized coordinate space. The portions of the mass matrix for PEA and SEA configurations corresponding to the generalized coordinates $\mathbf{q} = [x, y, \phi, \alpha, l]$ are identical except for one key difference. For a PEA at the hip, we must add the reflected motor inertia $j_{mot,\alpha}$ to the term corresponding to (α, α) (in this case M(4,4)), where $j_{mot,\alpha}$ is given by:

$$j_{mot,\alpha} = \frac{j_{unsc,\alpha}}{\bar{\dot{u}}_\alpha^2}. \tag{6}$$

In the above equation $j_{unsc,\alpha}$ is the unscaled inertia and $\bar{\dot{u}}_\alpha$ is the no-load speed of the motor. To avoid repetition, we refer the reader to our previous work [5] for details on these terms. Similarly, for a PEA at the leg, we must add the reflected motor inertia $j_{mot,l}$ to the term corresponding to (l, l) (in this case M(5,5)), where $j_{mot,l}$ is obtained by replacing α with l in Eqn. (6).

C. Cost Functions

To compare the efficiency of different combinations of the two actuator types for a 2D monoped hopping over a range of forward velocities, three cost functions are utilized to quantify the cost of transport. For each optimization we fix the average forward hopping speed $\dot{x}_d$ and quantify the cost of transport. All of the cost functions can then be expressed as an integral over the stride time ($t = 0$ until $t = T$). The COT is obtained by dividing the energy consumption in one stride by the total weight of the model and the distance it traveled over the duration T of that stride.

1) Positive Motor Work: By minimizing the positive motor work, we minimize the sum of the total energetic losses in the contact collisions, viscous damping in the springs, and negative motor work [9]. For the SEA, the total motor work for a single stride is given by:

$$\begin{aligned} c_{mot,l,SEA} &= \int_0^T max\left(F_{mot} \cdot \dot{u_l}, 0\right) dt \\ c_{mot,\alpha,SEA} &= \int_0^T max\left(T_{mot} \cdot \dot{u_\alpha}, 0\right) dt, \end{aligned} \tag{7}$$

In the case of the PEA, the actuator velocities are the same as the joint velocities. At any moment, the joint power is equal to the generalized joint force multiplying the joint velocities. Therefore the positive motor work ($c_{mot,l,PEA}$, $c_{mot,\alpha,PEA}$) can be calculated by replacing $\dot{u_l}$ and $\dot{u_\alpha}$ with $\dot{l}$ and $\dot{\alpha}$ respectively.

For all actuation configurations, the final cost function for one stride is the summation of the positive motor work at both the hip and knee joint.

2) Electrical Losses: The electrical losses represent the thermal losses in the motor. For both the parallel and series cases, the thermal losses in a single stride can be quantified as:

$$c_{loss} = \int_0^T \left(\frac{\bar{\dot{u}}_l^2}{P_{max,l}} F_{mot}^2 + \frac{\bar{\dot{u}}_\alpha^2}{P_{max,\alpha}} T_{mot}^2\right) dt \tag{8}$$

where $P_{max,l}$ and $P_{max,\alpha}$ represent the maximal motor power in the leg and hip motors respectively.

3) Electrical Work: We can also combine the two previous cost functions and balance the trade-off between motor work and thermal losses by using a more sophisticated cost function, the positive electrical work. This cost function is unique in that it allows negative work in one motor to be used to perform positive work or compensate for losses in another. For the series hip series leg case, the cost function is:

$$c_{el,SEA,SEA} = \int_0^T max\left(F_{mot} \cdot \dot{u_l} + T_{mot} \cdot \dot{u_\alpha} + \frac{\bar{\dot{u}}_l^2}{P_{max,l}} F_{mot}^2 + \frac{\bar{\dot{u}}_\alpha^2}{P_{max,\alpha}} T_{mot}^2, 0\right) dt \tag{9}$$

Authorized licensed use limited to: Technische Universitaet Muenchen. Downloaded on December 30,2021 at 10:34:46 UTC from IEEE Xplore. Restrictions apply.

For a parallel hip, $\dot{u_\alpha}$ is replaced with $\dot{\alpha}$. For a parallel leg, $\dot{u_l}$ is replaced with $\dot{l}$.

D. Optimization

We use optimal control to find energetically economical motions for each of the three cost functions (expressed as COT). In these optimizations we enforced periodic boundary conditions in order to obtain a continuous hopping motion. The motion obtained represents the ideal energetic cost, obtained during uninterrupted locomotion without outside disturbances. The results are therefore the upper bound on energetic economy. They do not take into account the additional energetic cost associated with stabilizing feedback.

We obtain optimal motor input by conducting velocity parameter studies using the multiple shooting optimization package MUSCOD [18]. MUSCOD provides a continuous piecewise linear motor input profile that minimizes the chosen cost function. For each point in these parameter studies, we fix the velocity, but leave morphological parameters as free variables. We include the hip and leg stiffness (k_α, k_l), the no load speeds of the hip and leg motors $(\bar{u}_\alpha, \bar{u}_l)$, the apex height of the main body, and for PEA, the hip and leg motor offset $(u_{offset,l}, u_{offset,\alpha})$ directly in the optimization. The bounds on these parameters (given in Table I) ensure that their values are realistic. The optimal motion is then obtained by integration of the equations of motion (Eqn. (5)). The above procedure is repeated for each actuator configuration and each cost function.

To ensure that the motions also remained realistic, we implemented constraints on the motion and motor input. The leg length was constrained to be $0.5l_o \leq l \leq 1.15l_o$. For SEA, the leg motor position was constrained to $-0.15l_o \leq u_l \leq 0.15l_o$. Additionally, the hip motor position was constrained to $-\pi/4 \leq u_\alpha \leq \pi/4$. For the motors we utilize the thermal loss conversion factor c_{lim}, which limits the available motor power to avoid overheating. For the SEA leg motor we have:

$$|F_{mot}| \leq c_{lim,l} \frac{P_{max,l}}{\bar{u}_l}, \tag{10}$$

and

$$|\dot{u}_l| \leq \bar{u}_l \left(1 - c_{lim,l}\right). \tag{11}$$

A detailed derivation of these equations can be found in Chapter 4.1.4 of [19]. For the SEA hip motor, l is replaced by α. For PEA, $\dot{u}_l$ is replaced by $\dot{l}$ and $\dot{u}_\alpha$ is replaced by $\dot{\alpha}$.

III. Results

We found that the optimal actuator configuration is both velocity dependent, and dependent on the cost function.

For the positive motor work COT, the optimal configuration was parallel for the hip and series for the leg (Fig. 2,a). That configuration has similar COT values to the other configurations at low velocities ($v < 0.325\sqrt{l_o g}$), but excels as velocity increases. For intermediate velocities, the monopeds with serial legs outperform those with parallel legs significantly. At a velocity of $v = 1.025\sqrt{l_o g}$ the serial leg monopeds have roughly the same COT (0.197). The monoped with a serial hip and parallel leg has a cost that is 13.86% higher, and the parallel hip parallel leg

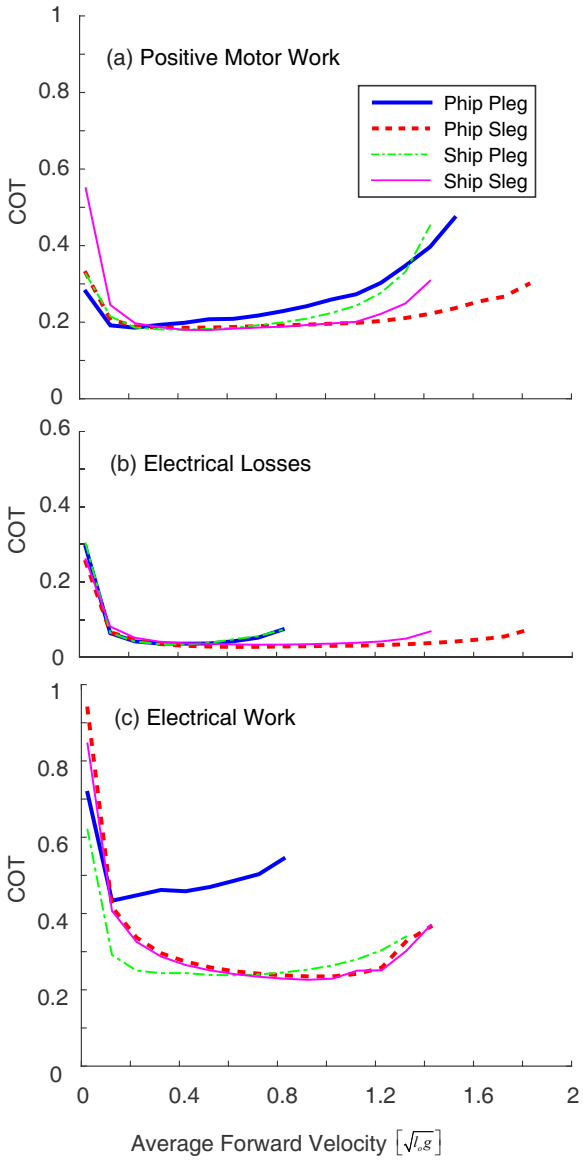

Fig. 2. A comparison of cost values for each actuator configuration. For the positive motor work and electrical loss COTs, the parallel hip and series leg configuration is energetically optimal. This configuration has the lowest cost throughout much of the velocity range. It also has the most solutions, indicating that it is able to meet realistic motor constraints at the most velocities. For the positive electrical work COT, there is no clear consensus on the optimal configuration. Series hip and parallel leg is optimal at low velocities, and both series hip series leg and parallel hip series leg are optimal at high velocities.

configuration has a cost that is 31.68% higher. At high velocities ($v > 1.125\sqrt{l_o g}$), the monopeds with series legs diverge in COT value, with the parallel hip and series leg becoming significantly more economical. At a velocity of $v = 1.425\sqrt{l_o g}$), the last solution found by the optimizer for the serial hip and serial leg, the monoped has a cost that is 38.72% higher than the parallel hip and series leg monoped. The optimizer found solutions for the PEA hip and SEA leg configuration at larger velocities (up to $v = 1.825\sqrt{l_o g}$) than the other configurations. The second highest velocity solution was found for PEA leg and PEA hip ($v = 1.525\sqrt{l_o g}$). The optimality of the series leg and parallel hip configuration stems primarily from low damping losses and negative motor

Authorized licensed use limited to: Technische Universitaet Muenchen. Downloaded on December 30,2021 at 10:34:46 UTC from IEEE Xplore. Restrictions apply.

work, with collisions playing a small role (Fig. 3,b). Fig. 3 also shows that both of the series leg configurations have significantly lower damping losses than the parallel leg configurations at high velocities.

For the electrical losses COT, the optimal configuration is again a PEA at the hip and a SEA at the leg (Fig. 2,b). As for the positive motor work, at low velocities ($v < 0.325\sqrt{l_o g}$), all of the configurations have nearly the same cost. At the last feasible solution for the parallel hip and parallel leg configuration ($v = 0.825\sqrt{l_o g}$), the monoped has a cost that is 153% higher than the parallel hip and series leg configuration. Additionally, the latter configuration had the most solutions found by the optimizer, with solutions found up to a velocity of $v = 1.825\sqrt{l_o g}$. The second highest velocity solution was found for the series leg and series hip monoped at $v = 1.425\sqrt{l_o g}$.

For the electrical work COT, there is no clear choice for the best configuration (Fig. 2,c). At low velocities, the series hip and parallel leg configuration is optimal, while at high velocities both the parallel hip series leg and series hip series leg monopeds are optimal (with both obtaining nearly the same cost).

IV. Discussion & Conclusion

In this paper, we apply optimal control to find the most energetically economical configuration of parallel and series elasticity on a two-dimensional monoped. In this process, we simultaneously optimize for motion and morphology. Not only do we compare the four different configurations of SEAs and PEAs, but we also optimize the springs, motor parameters, and motor offsets for each configuration. In addition, we enforce realistic constraints on leg length as well as motor force and velocity. We can therefore confidently say that we are comparing a realistic version of the best possible case for each configuration. Using these techniques, we have shown that for the positive motor work COT and the electrical losses COT, having a parallel hip and a series leg is the optimal configuration. For the positive electrical work, there is no consensus on the optimal choice.

While our optimal configuration prediction for the positive motor work COT was correct, our hypothesis proved incorrect for the other two COT. For electrical losses, this is not particularly surprising. For in-place hopping, the difference in optimal electrical losses for a serial leg compared to a parallel leg is small relative to the other cost functions [5]. It is therefore conceivable that the additional constraints and free parameters implemented here could lead to a shift in the optimal leg spring choice. For the positive electrical work, however, the result is entirely unexpected. The positive electrical work represents a combination of the positive motor work and the electrical losses. As the parallel hip and series leg is optimal for both positive motor work and electrical losses, it would seem that it should also be optimal for the positive electrical work. The discrepancy can likely be attributed to the fact that the cost function allows the negative work in one motor to be used to perform positive work or compensate for losses in the other. As this quality is

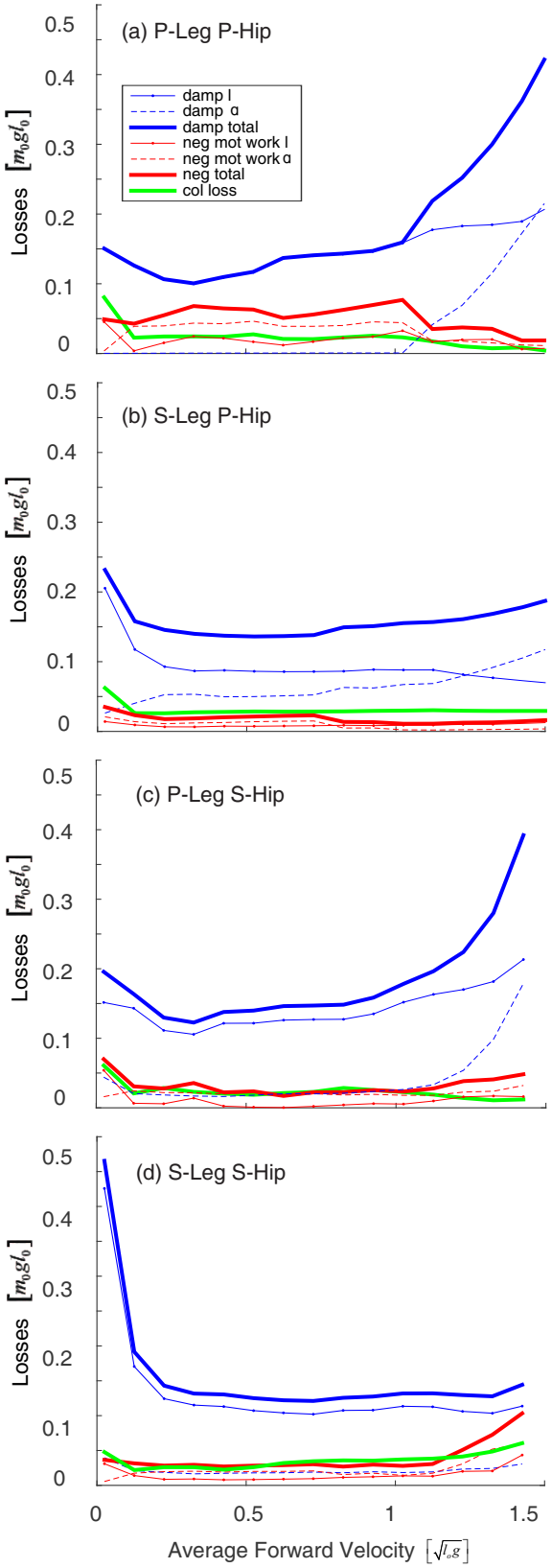

Fig. 3. The sources of losses for the positive motor work COT of all actuator configurations. The losses can come from damping in the leg and hip springs, negative motor work in the leg and hip motors, and collision losses. The losses primarily come from damping. Collision losses are generally small in comparison. The influence of negative motor work varies among the configurations.

Authorized licensed use limited to: Technische Universitaet Muenchen. Downloaded on December 30,2021 at 10:34:46 UTC from IEEE Xplore. Restrictions apply.

not present for the positive motor work, the positive electrical work does not accurately represent a combination of the other two cost functions.

For both the electrical losses and the positive motor work COT, the optimizer was able to find solutions at higher velocities than the other configurations. At higher velocities there are increased motor torques and velocities, as well as increased leg contraction and extension. The limiting factors to finding solutions therefore become the motor and leg length constraints. That fact implies that the series leg parallel hip configuration is best able to choose motion strategies that avoid these constraints. As for the one-dimensional hopper [5], this is a surprising result. The main advantage of PEA is that the spring and motor torques act additively (Eqns. 2,1). It would seem that therefore the PEA hip and the PEA leg would have a lower electrical loss COT, particularly at higher velocities where torques are much larger. Despite this, the PEA hip and SEA leg configuration has lower costs at nearly all velocities.

For the positive motor work, the series leg configurations have lower damping losses at higher speeds (Fig. 3). At first, it would seem that these losses are accounted for by the monoped's ability to use the motor position to decrease the rate of leg extension and compression(as in [5] for the one-dimensional hopper). At a closer look, however, the situation is more complex. The rapid increase in damping losses for the parallel leg configurations is driven by an increase in damping losses at the hip at high velocities. The damping loss increase occurs simply because at higher velocities, the leg is required to swing faster. The fact the the increase is steeper for the PEA leg configurations implies that there is an inherent coupling that occurs between actuators when there is a PEA at the leg. That is, the PEA at the leg is very sensitive to the timing of the leg oscillation. The choice of leg spring and leg motor mass therefore inherently sets a timing which the hip spring must adhere to. This coordination evidently leads to non-ideal hip motion, driving up hip costs. The series leg series hip configuration has lower damping losses than the series leg and parallel hip configuration at high velocities. Despite this, the lower negative motor work at high velocities required for the latter configuration drives down its overall cost.

In this work, we simultaneously consider a wide variety of parameters and constraints in a single optimization. This wide-ranging study comes at the expense of a detailed understanding of the fundamental effects of these design choices. As changing the parameters simultaneously influences the *natural dynamics* of the system, as well as the constraints, it is nearly impossible to extricate the effect of any one change on the system. For example, changing the no load speed in the hip motor will change the reflected motor inertia (Eqn. 6), which will in turn affect the motor dynamics for both PEA and SEA, collision losses for PEAs, and the ability to store energy in the motor for SEAs. Additionally, changing the no load speed changes the torque and velocity limits of the motors (Eqns. 10,11), directly affecting the constraints and limiting the possible motion. Every parameter changes the natural dynamics while simultaneously curtailing them (either by affecting the robots interaction with the constraints or the constraints directly).

While a fundamental understanding of the effect of PEA and SEA on two-dimensional legged locomotion is valuable and necessary, it was not our goal here. Instead, we showed that a complex and realistic design question for future hardware can be answered using optimal control. Despite the interplay of complicated motion and morphology, our optimization methodology was able to give insight into the best design choices.

REFERENCES

[1] Z. Gan, T. Wiestner, M. A. Weishaupt, N. M. Waldern, and C. D. Remy, "Passive dynamics explain quadrupedal walking, trotting, and tölting," *Journal of Computational and Nonlinear Dynamics*, 2015.

[2] H. Geyer, A. Seyfarth, and R. Blickhan, "Compliant leg behaviour explains basic dynamics of walking and running," *Proceedings of the Royal Society B*, vol. 273, no. 1603, pp. 2861–2867, 2006.

[3] M. P. McGuigan and A. M. Wilson, "The effect of gait and digital flexor muscle activation on limb compliance in the forelimb of the horse equus caballus," *Journal of Experimental Biology*, vol. 206, no. 8, pp. 1325–1336, 2003.

[4] R. M. Alexander, "Three uses for springs in legged locomotion," *The International Journal of Robotics Research*, vol. 9, no. 2, pp. 53–61, 1990.

[5] Y. Yesilevskiy, W. Xi, and C. D. Remy, "A comparison of series and parallel elasticity in a monoped hopper," in *2015 IEEE International Conference on Robotics and Automation (ICRA)*, pp. 1036–1041, IEEE, 2015.

[6] A. D. Kuo, "Choosing your steps carefully," *Robotics & Automation Magazine, IEEE*, vol. 14, no. 2, pp. 18–29, 2007.

[7] G. Gabrielli and T. Von Karman, *What price speed?: specific power required for propulsion of vehicles*. 1950.

[8] V. A. Tucker, "The energetic cost of moving about: Walking and running are extremely inefficient forms of locomotion. much greater efficiency is achieved by birds, fishand bicyclists," *American Scientist*, vol. 63, no. 4, pp. 413–419, 1975.

[9] C. D. Remy, K. Buffinton, and R. Siegwart, "Comparison of cost functions for electrically driven running robots," in *2015 IEEE International Conference on Robotics and Automation (ICRA)*, pp. 2343–2350, IEEE, 2012.

[10] M. Gomes and A. Ruina, "Walking model with no energy cost," *Physical Review E*, vol. 83, no. 3, p. 032901, 2011.

[11] M. Hutter, C. D. Remy, M. A. Hoepflinger, and R. Siegwart, "Scarleth: Design and control of a planar running robot," in *Intelligent Robots and Systems (IROS), 2011 IEEE/RSJ International Conference on*, pp. 562–567, IEEE, 2011.

[12] J. Grizzle, J. Hurst, B. Morris, H.-W. Park, and K. Sreenath, "Mabel, a new robotic bipedal walker and runner," in *American Control Conference, 2009. ACC'09.*, pp. 2030–2036, IEEE, 2009.

[13] J. D. Karssen, M. Haberland, M. Wisse, and S. Kim, "The effects of swing-leg retraction on running performance: analysis, simulation, and experiment," *Robotica*, vol. 33, no. 10, pp. 2137–2155, 2015.

[14] M. Grimmer, M. Eslamy, S. Gliech, and A. Seyfarth, "A comparison of parallel-and series elastic elements in an actuator for mimicking human ankle joint in walking and running," in *2015 IEEE International Conference on Robotics and Automation (ICRA)*, pp. 2463–2470, IEEE, 2012.

[15] J. James, P. Ross, and D. Ball, "Comparison of elastic configurations for energy efficient legged locomotion,"

[16] W. Xi, Y. Yesilevskiy, and C. D. Remy, "Selecting gaits for economical locomotion of legged robots," *The International Journal of Robotics Research*, 2015.

[17] C. D. Remy, K. Buffinton, and R. Siegwart, "A matlab framework for efficient gait creation," in *Intelligent Robots and Systems (IROS), 2011 IEEE/RSJ International Conference on*, pp. 190–196, IEEE, 2011.

[18] M. Diehl, D. B. Leineweber, and A. A. Schäfer, *MUSCOD-II User's Manual*. IWR, 2001.

[19] C. D. Remy, *Optimal Exploitation of Natural Dynamics in Legged Locomotion*. PhD thesis, Eidgenssische Technische Hochschule, 2011.

Authorized licensed use limited to: Technische Universitaet Muenchen. Downloaded on December 30,2021 at 10:34:46 UTC from IEEE Xplore. Restrictions apply.